

## Environmental factors controlling the Barents Sea spring-summer phytoplankton blooms

Sergio R. Signorini<sup>1</sup> and Charles R. McClain<sup>2</sup>

Received 10 February 2009; revised 11 April 2009; accepted 24 April 2009; published 29 May 2009.

[1] We provide an analysis of the seasonal change of the physical forcing factors and their impact on the timing and intensity of phytoplankton blooms in the Barents Sea, with emphasis on the different functional groups that can be distinguished (coccolithophores and other phytoplankton groups) using satellite remote sensing algorithms. Our analyses are based on an integration of satellite derived products and historical hydrographic data. There is a significant phase shift between the peaks of the diatom bloom in May to the coccolithophore bloom in August. Light and nutrient variability, driven by the large seasonal changes of solar irradiance and mixed layer depth in the Barents Sea, are the major environmental factors controlling these phytoplankton blooms. Based on previous field campaigns that identified *Emiliana huxleyi* as the most predominant species of coccolithophores in the Barents Sea, we conclude that the high concentration of calcite retrieved by ocean color satellites in summer is a result of bloom-forming coccolithophores of this species. A strong correlation between calcite concentration and wind speed squared ( $r^2 = 0.8$ ) was found during the peak of the bloom. We suggest that this correlation is an indication of CO<sub>2</sub> fertilization resulting from regionally enhanced uptake of atmospheric CO<sub>2</sub>. **Citation:** Signorini, S. R., and C. R. McClain (2009), Environmental factors controlling the Barents Sea spring-summer phytoplankton blooms, *Geophys. Res. Lett.*, 36, L10604, doi:10.1029/2009GL037695.

### 1. Introduction

[2] The Barents Sea is a shallow marginal sea of the Arctic Ocean with connections to the Norwegian Sea to the west and the Kara Sea to the east. From January through June, and November – December, the eastern Barents Sea is mostly ice covered, while in August – September most of the region south of 80°N is ice free. Figure 1a shows climatologic (1955–2006) sea-surface temperature (SST) and surface currents for August adapted from multi-decadal simulations of a coupled ice-ocean model of the Arctic Ocean [Häkkinen and Proshutinsky, 2004]. The Norwegian Atlantic Current (NwAC) transports relatively warm and salty North Atlantic water northeastward from the Norwegian Sea into the Barents, while southward-flowing currents to the east of Svalbard (Persey and east Spitsbergen currents) transport colder and fresher water of Arctic origin southward into the Barents [Harris et al., 1998; Ingvaldsen,

2005]. The merging of these currents forms the polar front identified by the strongest horizontal gradients, usually between 3° and 4°C isotherms at 50 meters [Johannessen and Foster, 1978]. The part of the NwAC that flows northward and parallels the coast west of Svalbard is called West Spitsbergen Current. The part of the NwAC that enters the Barents Sea is called North Cape Current (NCaC). The NCaC splits into two main branches in the western Barents, one branch continues eastward parallel to the coast while the other turns north. The path and convergence of all these currents reflects on the SST distribution shown in Figure 1a. Strong winds and convective overturning promote deep mixed layers in winter, while restratification occurs in summer due to ice melt and the warming of surface waters as a result of increased solar radiation. This very dynamic physical forcing has a significant impact on the seasonal and interannual cycles of phytoplankton species of the Barents Sea. Light availability, ice cover, vertical mixing, the location of the polar front, and SST change significantly from winter to spring and summer, which are the primary environmental factors controlling the Barents Sea spring-summer phytoplankton blooms [Kogeler and Rey, 1999]. Here we provide an analysis of the seasonal change of the physical forcing factors and their impact on the timing and intensity of phytoplankton blooms, with emphasis on the different functional groups that can be distinguished (coccolithophores and other phytoplankton groups) using satellite remote sensing algorithms. Coccolithophores, among which *E. huxleyi* is the most abundant and widespread species, are considered to be the most productive calcifying organism on earth. They are important components of the carbon cycle via their contribution and response to changes in atmospheric CO<sub>2</sub> levels.

[3] Our analyses are based on an integration of satellite derived products (Chl-a, calcite, SST, and ice concentration) and historical hydrographic data.

### 2. Data Sources and Methodology

[4] We used 9-km Level 3 monthly composites of MODIS-Aqua (MODISA) Chl-a, Calcite, SST, and SeaWiFS PAR (<http://oceancolor.gsfc.nasa.gov>). Sea ice concentration was obtained from SSM/I 25-km monthly composites provided by Don Cavalieri and model products to derive climatologic SST and surface currents (see Figure 1a) were obtained from Sirpa Häkkinen (NASA's Cryospheric Sciences Branch). Monthly mixed layer depth was obtained from the NOAA/OAR/ESRL PSD, Boulder, Colorado, USA (<http://www.cdc.noaa.gov>), and the monthly nutrient concentrations from the World Ocean Atlas 2005 [Garcia et al., 2006]. We obtained temperature, salinity, and nutrient profiles from 2164 stations in the Barents Sea from the

<sup>1</sup>Sciences Applications International Corporation, Beltsville, Maryland, USA.

<sup>2</sup>NASA Goddard Space Flight Center, Greenbelt, Maryland, USA.

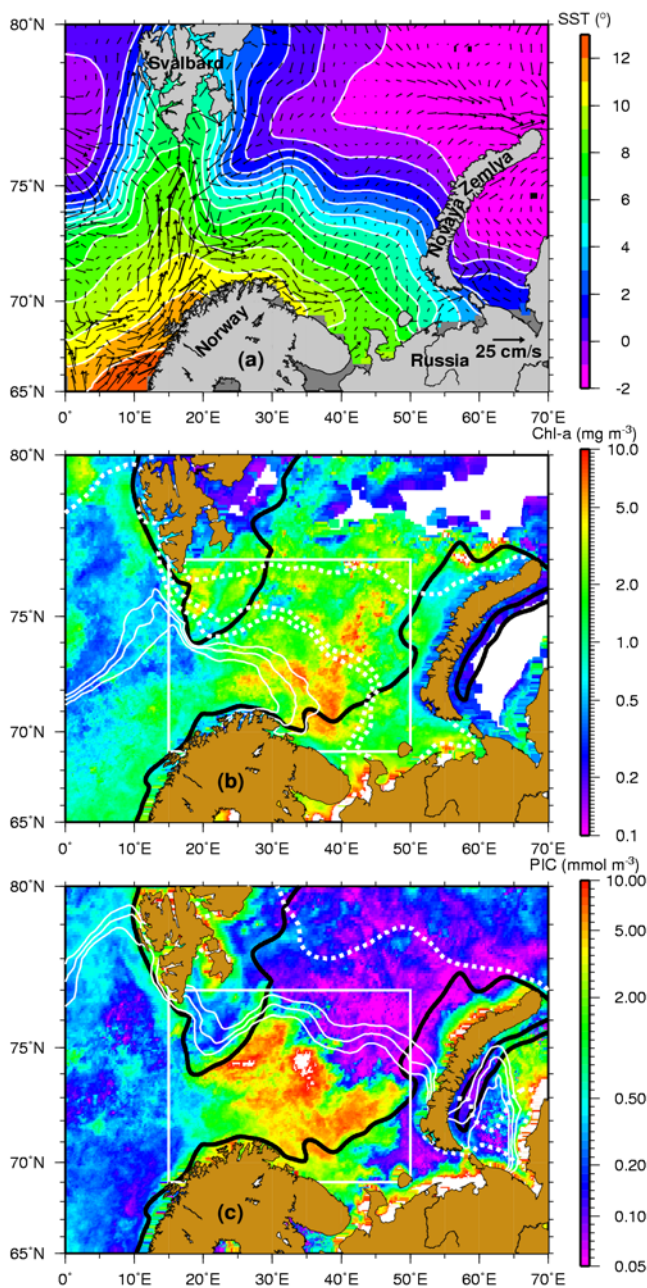


**Figure 1.** (a) Barents Sea climatologic SST and surface currents for August derived from 50 years (1955–2005) of coupled ice-ocean model simulation [Häkkinen and Proshutinsky, 2004]. Climatologic monthly composites of (b) MODIS Chl-a for May and (c) calcite for August. See text for explanation.

NODC's World Ocean Database (<http://www.nodc.noaa.gov/OC5/SELECT/dbsearch/dbsearch.html>). Mixed layer depths (MLD) were derived from each profile using a potential density threshold of  $0.01 \text{ kg m}^{-3}$  [Thomson and Fine, 2003].

[5] The energy available for biological production is dependent on day length, solar inclination, cloud cover and ice cover. In the Arctic, due to lower sun angles, light intensity and color are more influenced by the atmosphere than in more temperate regions. Typically, the Barents Sea region is 80% cloud covered during the summer months

[Rossow and Schiffer, 1999]. Although this may bias the time binning of ocean color satellite products, only a few clear scenes are required over a whole season to determine if a bloom has occurred. Furthermore, our analysis is based on monthly climatology composites, which render the seasonal variability more statistically robust. The chlorophyll algorithm flags ice and clouds in the same manner and retrieves Chl-a only in open areas of the ice field. The calcite algorithm is not capable of distinguishing PIC from ice. However, during the coccolithophore bloom season (July – September) the Barents Sea is mostly ice free. The binning of the Chl-a product is obtained by excluding pixels for which coccolithophores are flagged using reflectance thresholds. This process precludes the estimation of presumably lower levels of Chl-a associated with the coccolithophore blooms.

### 3. Discussion and Results

[6] The Barents Sea ecosystem has been previously studied using a variety of observing methods. Mitchell *et al.* [1991] studied the meridional zonation of the Barents Sea ecosystem using a combination of satellite ocean color data and in situ bio-optical observations. Their findings showed that massive blooms of subsurface phytoplankton embedded in the pycnocline persist throughout the summer and maintain substantial rates of primary production. Smyth *et al.* [2004] used a combination of several visible band satellite radiometers to analyze a multi-decadal time series of coccolithophore activity in the Barents Sea. They concluded that coccolithophores appear to be advancing into some sub-Arctic Seas and that climate change induced warming and freshwater runoff may be causing an increased frequency of coccolithophore blooms within the Barents Sea. In situ sampling at  $73^{\circ}36'N$ ,  $26^{\circ}48'E$  during August 2003 confirmed the presence of high concentrations of *Emiliana huxleyi* coccoliths corresponding to bright water seen in ocean color satellite imagery [Smyth *et al.*, 2004]. This location is within the same area where the highest calcite concentrations were observed in August images analyzed in our study. *E. huxleyi* blooms have also been observed near the marginal ice zone of the northern Barents Sea ( $80 - 81^{\circ}N$ ,  $30^{\circ}E$ ) in August 2003 down to 50 m, which have been attributed to intrusions of water of Atlantic origin bringing cells of oceanic phytoplankton species via the subsurface circumpolar boundary current west of Svalbard and then eastward along the Eurasian Shelf break [Hegseth and Sundfjord, 2008]. Large numbers of diatoms were also identified in these blooms.

[7] In the southern Barents Sea, where the Atlantic water masses are dominant, both the increase in light intensity and day length and the increasing vertical stability of the water masses are important for the timing of the spring bloom [Eilertsen *et al.*, 1993]. The bloom usually starts in April and can last until May or June. In the northern Barents Sea, the phytoplankton bloom first starts after the ice has melted. The stable surface layer that is formed lasts the whole growing season with a strong pycnocline which inhibits exchange of nutrients. As a result, intense ice edge blooms develop very rapidly. The bloom stops abruptly when nutrients in the layer become depleted, causing the chlorophyll maximum to sink to greater depths [Mitchell *et al.*,

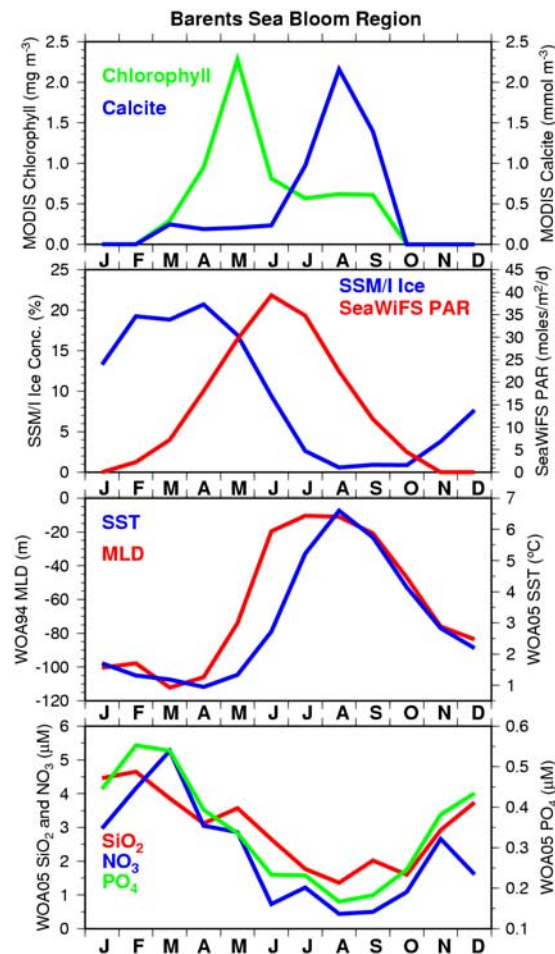


**Figure 2.** Seasonal time series of physical and biogeochemical parameters averaged within the white boxes shown in Figures 1b and 1c.

1991; Rey and Loeng, 1985]. Here we focused on the southern Barents Sea where we were able to distinguish the spring bloom, which peaks in May and presumably consisting of diatoms and flagellates detected by the Chl-a algorithm, from the summer coccolithophore bloom that peaks in August and detected by the calcite algorithm in the region immediately north of Norway.

[8] Figure 1 shows MODISA climatologic composites of Chl-a for May (Figure 1b) and PIC for August (Figure 1c). The three white contour lines represent the 4, 4.5, 5°C SST isotherms derived from MODISA SST, which indicate the region of strongest horizontal SST gradients and a proxy for the location of the polar front. Black lines in 1b and 1c represent the 200 m isobaths. The rectangle bound by the white lines indicates the region of highest concentrations of Chl-a and PIC. The three white dashed lines in Figure 1b are the 10%, 20% and 50% ice concentration contours for May, while the dashed line in Figure 1c is the 10% ice concentration line for August, indicating a northward retreat of the ice edge. The bloom area with Chl-a values exceeding  $2 \text{ mg m}^{-3}$  in May, as well as the bloom area exceeding  $2 \text{ mmol m}^{-3}$  of PIC in August, approaches  $10,000 \text{ km}^2$ . During these months of most intense blooms, Chl-a and PIC concentrations exceed 10 units in the most productive areas. The spring bloom in May is more intense on the cooler side of the polar front and penetrates into the ice field to the north. Conversely, in August, when the polar front and ice edge move northward, the highest PIC concentrations are confined within the southern (warmer side) of the polar front. This behavior is quite unique and it is the focus of our more detailed analysis described below.

[9] Figure 2 shows the response of the southern Barents Sea ecosystem to seasonal physical forcing and nutrient availability. All parameters were averaged within the boxes shown in Figure 1 and monthly averages are shown in Table 1. The classic pattern of the onset of spring bloom is clearly shown in Figure 2. Chl-a concentrations begin to rise in March following the increase of light availability (PAR) and a distinct drawdown of nutrients ensues. As solar irradiance continues to increase, there is a sharp decrease in the average MLD from March to May ( $\sim 100 \text{ m}$  to  $\sim 70 \text{ m}$ ) accompanied by further drawdown of nutrients during which the Chl-a reaches a peak. Further decrease in the MLD ( $< 20 \text{ m}$ ) in June, and most likely grazing by the herbivore population, causes a significant drop in the average Chl-a ( $> 2 \text{ mg m}^{-3}$  to  $< 1 \text{ mg m}^{-3}$ ). The average Chl-a levels are  $\sim 0.7 \text{ mg m}^{-3}$  in July and drop to zero after September when solar irradiance is significantly reduced. Surface cooling and stronger winds deepen the MLD and nutrient levels begin to increase again via vertical mixing during the winter months.

**Table 1.** Monthly Means of SST, SSS, Ice Concentration, MLD, PAR, Silicate, Nitrate, Phosphate, Chl-a, and Calcite<sup>a</sup>

Month	SST (°C)	SSS (psu)	Ice (%)	MLD (m)	PAR (moles $\text{m}^{-2} \text{d}^{-1}$ )	SiO <sub>2</sub> (μM)	NO <sub>3</sub> (μM)	PO <sub>4</sub> (μM)	Chl-a (mg $\text{m}^{-3}$ )	PIC (mmol $\text{m}^{-3}$ )
Jan	1.7	34.70	13.3	100.4	0.0	4.5	3.0	0.45	0.0	0.0
Feb	1.3	34.72	19.3	97.8	2.3	4.7	4.2	0.55	0.0	0.0
Mar	1.2	34.72	18.8	112.2	7.2	3.9	5.3	0.54	0.29	0.25
Apr	0.9	34.67	20.7	106.0	18.1	3.1	3.1	0.39	0.95	0.19
May	1.3	34.64	16.9	74.0	29.5	3.6	2.9	0.34	2.28	0.21
Jun	2.7	34.46	9.4	19.7	39.3	2.7	0.7	0.23	0.81	0.24
Jul	5.2	34.27	2.6	10.4	34.8	1.8	1.2	0.23	0.57	0.97
Aug	6.6	34.25	0.6	11.0	27.5	1.4	0.4	0.17	0.62	2.16
Sep	5.7	34.33	0.9	20.8	11.8	2.0	0.5	0.18	0.61	1.39
Oct	4.1	34.45	0.9	47.0	4.5	1.6	1.1	0.25	0.0	0.0
Nov	2.8	34.41	3.8	75.9	0.0	2.9	2.7	0.38	0.0	0.0
Dec	2.2	34.67	7.7	83.5	0.0	3.7	1.6	0.44	0.0	0.0

<sup>a</sup>Monthly averages within box in Figures 1b and 1c.



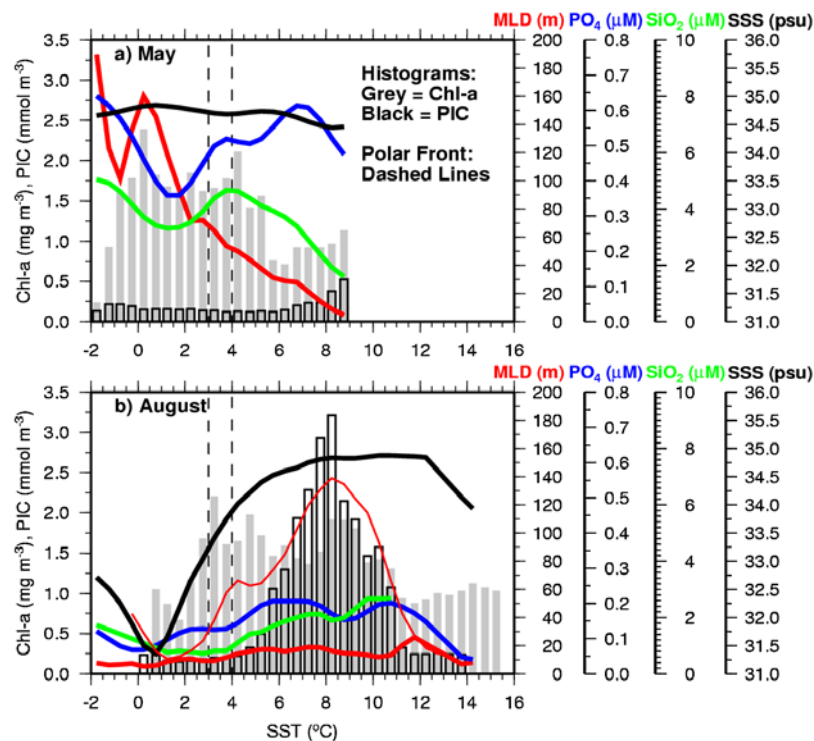


**Figure 3.** Histograms of physical and biogeochemical parameters in the Barents Sea ( $0^{\circ}\text{E}$ – $70^{\circ}\text{E}$ ,  $65^{\circ}\text{N}$ – $80^{\circ}\text{N}$ ) for (a) May and (b) August. All parameters are averaged within  $0.5^{\circ}\text{C}$  SST bins across the whole range of observed SSTs.

[10] The seasonal phasing of the coccolithophore bloom, identified here by the variability in calcite concentration retrieved by satellite, is quite different from the seasonal phasing of the “other phytoplankton” (e.g., diatoms and flagellates), described above using the satellite Chl-*a*. It is well known that high light conditions trigger *E. huxleyi* blooms [Nanninga and Tyrrell, 1996; Tyrrell and Merico, 2004]. Reports of natural blooms of *E. huxleyi* reveal that they all occur in highly stratified water where the MLD is usually  $\sim 10$ – $20$  m, and is always  $\leq 30$  m [Nanninga and Tyrrell, 1996]. Figure 2 and Table 1 show a sharp rise in PIC concentration beginning in July and peaking in August. The average MLD in July and August are the shallowest of the entire year (10.4 to 11 m) and August has the warmest SST ( $6.6^{\circ}\text{C}$ ). August is also the month with least ice cover (0.6%), freshest surface water (34.25 psu), and most nutrient depleted surface waters ( $\text{SiO}_2 = 1.4 \mu\text{M}$ ,  $\text{NO}_3 = 0.4 \mu\text{M}$ , and  $\text{PO}_4 = 0.17 \mu\text{M}$ ). This combination of environmental factors seems to be conducive to the highest calcite production by coccolithophores in the southern Barents Sea. In general, blooms of *E. huxleyi* follow those of diatoms in waters that have been recently depleted in inorganic nutrients and are becoming more stable in terms of vertical mixing [Holligan et al., 1993]. This is certainly our own conclusion in the Barents Sea, and in previous studies in the Patagonia Shelf break [Garcia et al., 2008; Signorini et al., 2006].

[11] Further analyses for the entire Barents Sea reveals an interaction of the coccolithophore blooms with environmental factors, and their distinction in behavior from other functional groups. Figure 3 summarizes these analyses with histograms of physical and biogeochemical parameters as a function of SST, which is a good indicator of water mass

distribution (Atlantic versus Arctic origin) in the Barents Sea (see Figure 1a). Values were extracted for May and August from areas deeper than 200 m to reduce the influence of coastal waters (see Figure 1). The grey histograms are for Chl-*a*, while the black histograms are for PIC. The distributions of SSS, MLD, silicate and phosphate versus SST are shown as color-coded lines and the approximate location of the polar front is shown by the dashed lines. A distinct attribute shown by the histograms is that phytoplankton species identified by Chl-*a* are eurythermal and their growth seems to be controlled by nutrient availability during spring and summer, while the coccolithophores, identified here by the calcite concentration, are much more abundant at temperatures near  $8^{\circ}\text{C}$  in August, with a distinct Gaussian distribution around that temperature. In May, Chl-*a* values are higher ( $>1.5 \text{ mg m}^{-3}$ ) at colder temperatures ( $-1$  to  $4^{\circ}\text{C}$ ) with MLD deeper than 80 m and highest  $\text{SiO}_2$  and  $\text{PO}_4$  concentrations. The Chl-*a* values on the warmer side of the front are reduced ( $<1.0 \text{ mg m}^{-3}$ ) due to shallower MLDs and consumption of  $\text{SiO}_2$  by fast growing diatoms. In August, when surface waters become highly stratified (MLD  $< 20$  m) and inorganic nutrients become depleted but not exhausted, the coccolithophore bloom attains its peak and calcite production reaches the season’s maximum. The MLD is mostly controlled by higher SSTs on the warm side of the front and by reduced SSS via freshwater originating from ice melt on the cold side of the front. This results in shallow MLDs ( $<20$  m) across the whole Barents Sea. Despite shallow MLDs across the Barents, the calcite concentration is highest on the warm side of the front and peaks around  $8^{\circ}\text{C}$ . Water temperature, in combination with other parameters, appears to be a good predictor of *E. huxleyi* blooms which are associated with

water temperatures between 3°C and 15°C [Iglesias-Rodríguez et al., 2002]. Another parameter, the wind speed squared ( $W^2$  from NCEP-2 Reanalysis), was identified as a factor in the spatial distribution of the bloom ( $W^2$  is the thin red line in Figure 3b and ranges from 24 m<sup>2</sup> s<sup>-2</sup> to 76 m<sup>2</sup> s<sup>-2</sup>). Strong correlation ( $r^2 = 0.80$ ) was found between calcite concentration and  $W^2$  during the peak of the bloom in August. This is not a result of wind-enhanced vertical mixing as the correlation between PIC and MLD in SST space is very low (0.18). We hypothesize that the strong PIC versus  $W^2$  correlation is a result of CO<sub>2</sub> fertilization from regionally enhanced uptake of atmospheric CO<sub>2</sub>.

#### 4. Summary and Conclusions

[12] Since previous field campaigns identified *E. huxleyi* as the most predominant species of coccolithophores in the Barents Sea [Hegseth and Sundfjord, 2008; Smyth et al., 2004], we conclude that the high concentration of PIC retrieved by ocean color satellites in summer is a result of bloom-forming coccolithophores of this species. A distinction of functional groups is made by contrasting blooms of diatoms and flagellates [Hegseth and Sundfjord, 2008], identified by satellite Chl-a retrievals, from blooms of coccolithophores identified by satellite calcite retrievals. We have successfully applied this methodology before using in situ verification along the Patagonia Shelf break off of Argentina [Garcia et al., 2008; Signorini et al., 2006].

[13] There is a significant phase shift between the peaks of the diatom bloom in May to the coccolithophore bloom in August. Light and nutrient variability, driven by the large seasonal changes of solar irradiance and MLD in the Barents Sea, are the major environmental factors controlling these phytoplankton blooms. The distribution of the blooming diatoms is wide spread in spring-summer and are very abundant (high satellite Chl-a) even within low temperatures in open areas within the ice field, while the coccolithophores are much more abundant (high satellite PIC) in August during the peak of vertical stratification and after the diatoms have depleted the mixed layer inorganic nutrients.

[14] There is some evidence of possible climate change impacts on high latitude coccolithophore species. For example, predicted freshening of polar seas may increase stratification, thus favoring an increase in bloom development [Smyth et al., 2004]. In addition, the anthropogenic increase of atmospheric CO<sub>2</sub> may also have an impact on the coccolithophorid populations as a result of changes in the carbonate chemistry of seawater [Herfort et al., 2002; Iglesias-Rodríguez et al., 2002; Langer et al., 2006].

[15] There is a significant correlation between calcite concentration and  $W^2$  ( $r^2 = 0.8$ ) during the peak of the bloom. Although more detailed analysis are being conducted to evaluate its consequences, we hypothesize that this correlation is an indication of CO<sub>2</sub> fertilization resulting from regionally enhanced uptake of atmospheric CO<sub>2</sub>.

[16] **Acknowledgment.** This work was funded by the NASA Ocean Biology and Biogeochemistry Program.

#### References

- Eilertsen, H. C., et al. (1993), The onset of the spring phytoplankton bloom in the Barents Sea: Influence of changing light regime and other environmental factors, *Underwater Light Meas.*, 2048, 20–32.
- Garcia, H. E., et al. (2006), *World Ocean Atlas 2005*, vol. 4, *Nutrients (Phosphate, Nitrate, Silicate)*, 396 pp., U.S. Gov. Print. Off., Washington D. C.
- Garcia, V. M. T., et al. (2008), Environmental factors controlling the phytoplankton blooms at the Patagonia shelf-break in spring, *Deep Sea Res., Part I*, 55, 1150–1166.
- Häkkinen, S., and A. Proshutinsky (2004), Freshwater content variability in the Arctic Ocean, *J. Geophys. Res.*, 109, C03051, doi:10.1029/2003JC001940.
- Harris, C. L., A. J. Plueddemann, and G. G. Gawarkiewicz (1998), Water mass distribution and polar front structure in the western Barents Sea, *J. Geophys. Res.*, 103, 2905–2917.
- Hegseth, E. N., and A. Sundfjord (2008), Intrusion and blooming of Atlantic phytoplankton species in the high Arctic, *J. Mar. Syst.*, 74, 108–119.
- Herfort, L., et al. (2002), Acquisition and use of bicarbonate by *Emiliania huxleyi*, *New Phytol.*, 156, 427–436.
- Holligan, P. M., et al. (1993), What controls the distribution of the coccolithophore, *Emiliania huxleyi*, in the North Sea?, *Fish Oceanogr.*, 2, 175–183.
- Iglesias-Rodríguez, M. D., C. W. Brown, S. C. Doney, J. Kleypas, D. Kolber, Z. Kolber, P. K. Hayes, and P. G. Falkowski (2002), Representing key phytoplankton functional groups in ocean carbon cycle models: Coccolithophorids, *Global Biogeochem. Cycles*, 16(4), 1100, doi:10.1029/2001GB001454.
- Ingvoldsen, R. B. (2005), Width of the North Cape Current and location of the Polar Front in the western Barents Sea, *Geophys. Res. Lett.*, 32, L16603, doi:10.1029/2005GL023440.
- Johannessen, O. M., and L. A. Foster (1978), A note on the topographically controlled oceanic polar front in the Barents Sea, *J. Geophys. Res.*, 83, 4567–4571.
- Kogeler, J., and F. Rey (1999), Ocean colour and the spatial and seasonal distribution of phytoplankton in the Barents Sea, *Int. J. Remote Sens.*, 20, 1303–1318.
- Langer, G., M. Geisen, K.-H. Baumann, J. Kläs, U. Riebesell, S. Thoms, and J. R. Young (2006), Species-specific responses of calcifying algae to changing seawater carbonate chemistry, *Geochem. Geophys. Geosyst.*, 7, Q09006, doi:10.1029/2005GC001227.
- Mitchell, B. G., et al. (1991), Meridional zonation of the Barents Sea ecosystem inferred from satellite remote-sensing and in situ bio-optical observations, *Polar Res.*, 10, 147–162.
- Nanninga, H. J., and T. Tyrrell (1996), Importance of light for the formation of algal blooms by *Emiliania huxleyi*, *Mar. Ecol. Prog. Ser.*, 136, 195–203.
- Rey, F., and H. Loeng (1985), The influence of ice and hydrographic conditions on the development of phytoplankton in the Barents Sea, in *Marine Biology of Polar Regions and Effects of Stress on Marine Organisms*, edited by J. Gray and M. E. Christiansen, pp. 49–63, John Wiley, London.
- Rosow, W. B., and R. A. Schiffer (1999), Advances in understanding clouds from ISCCP, *Bull. Am. Meteorol. Soc.*, 80, 2261–2287.
- Signorini, S. R., V. M. T. Garcia, A. R. Piola, C. A. E. Garcia, M. M. Mata, and C. R. McClain (2006), Seasonal and interannual variability of calcite in the vicinity of the Patagonian shelf break (38°S–52°S), *Geophys. Res. Lett.*, 33, L16610, doi:10.1029/2006GL026592.
- Smyth, T. J., T. Tyrrell, and B. Tarrant (2004), Time series of coccolithophore activity in the Barents Sea, from twenty years of satellite imagery, *Geophys. Res. Lett.*, 31, L11302, doi:10.1029/2004GL019735.
- Thomson, R. E., and I. V. Fine (2003), Estimating mixed layer depth from oceanic profile data, *J. Atmos. Oceanic Technol.*, 20, 319–329.
- Tyrrell, T., and A. Merico (2004), *Emiliania huxleyi*: Bloom observations and the conditions that induce them, in *Coccolithophores: From Molecular Processes to Global Impact*, edited by H. R. Thierstein and J. R. Young, pp. 75–97, Springer, Berlin.

C. R. McClain, NASA Goddard Space Flight Center, Code 614.8, Greenbelt, MD 20771, USA. (charles.r.mcclain@nasa.gov)

S. R. Signorini, Sciences Applications International Corporation, 4600 Powder Mill Road, Beltsville, MD 20705-2675, USA. (sergio.signorini@nasa.gov)